Electron-Paramagnetic-Resonance Study of Clean and Oxygen-Exposed Surfaces of GaAs, AlSb, and Other III-V Compounds*

D. J. Miller and D. Haneman
School of Physics, University of New South Wales, Sydney, Australia, 2033
(Received 26 October 1970)

Clean surfaces of p-type GaP, GaAs, GaSb, and InAs and n-type GaAs, AlSb, and GaSb have been prepared by crushing in ultrahigh vacuum (10^{-9} Torr) and measured by the electron-paramagnetic-resonance technique at room temperature and 77 °K. A small clean-surface signal was found. When oxygen was adsorbed at 77 °K, a new signal was found, due to O_2^- ions. In the case of AlSb, hyperfine structure was resolved. A complete analysis was carried out without the usual restriction of setting the $\overleftrightarrow{A}$ (hyperfine) and $\overleftrightarrow{g}$ tensors parallel. Parameters were checked by computer simulations of the spectra. About 5% of the wave function of the unpaired electron on the O_2^- molecule is localized on the Al atom. The unfilled (dangling) orbital of this surface atom is found to be over 90% p type. This provides, apparently, the first experimental determination of a clean-semiconductor-surface wave function. A model of the (110) surface of a III-V compound semiconductor is proposed. The group-V atom dangling bond contains an electron pair in a p orbital, while the group-III atom dangling bond is a largely empty p orbital. In-surface bonds are largely sp^2. Parameters for the clean-surface signal on GaAs and GaSb are $g = 2.0038 \pm 0.0004$, width 10 ± 1 G, corresponding to about 4×10^{11} spins cm^{-2}, reduced by about 30% after exposure to air. For the O_2^- signal on GaAs $g_{\parallel} = 2.036$, $g_{\perp} = 2.007$, and on AlSb $g_{\parallel} = 2.041$, $g_{\perp} = 2.005$.

I. INTRODUCTION

This paper reports the results of measurements of surface wave functions and other properties of certain compound semiconductors by electron paramagnetic resonance (EPR). It was found that an EPR signal from oxygen weakly adsorbed at liquid-nitrogen temperatures was useful as a surface probe.

Many surfaces, mainly of semiconductors, have been studied by EPR, but relatively little work has been done on properly characterized clean surfaces. Information has been obtained about dangling bonds,[1-3] surface defects, and adsorbed species.[3-8] Of the III-V compounds, only GaAs and InAs[9,10] surfaces have been studied previously and no resonance was then reported from them. A signal was found after annealing[10,11] but this was later identified as due to carbon contamination.[11,12]

Powders crushed and measured in ultrahigh vacuum (uhv) have been used to provide large surface areas for sufficient sensitivity. Measurement sensitivity was improved by use of signal averaging techniques, in order to detect unpaired electrons which may correspond to only a small fraction of a monolayer. Since the EPR signals from cleaved and crushed silicon are nearly identical,[2] it is assumed the surfaces exposed by crushing are characteristic of the corresponding cleaved surface. Crushing exposes mainly (110) faces in the case of the III-V compounds.[13]

We report a small signal which apparently originates from the clean GaAs surface. In addition, a relatively intense signal is found after exposure of GaAs and AlSb powders to oxygen below room temperature. In Sec. IV, this signal is shown to be from O_2^- ions which others have found on the surfaces of SiO_2,[3] MgO,[4,6] ZnO,[4,5] and zeolites.[7,8] The signal from O_2^- ions adsorbed on AlSb shows hyperfine structure (hfs) due to interaction with a surface nucleus. This interaction takes place when the unpaired electron occupies a surface wave function which is found to be largely p-like. This is thought to be the first experimental determination of a surface wave function on a semiconductor. Other properties of the (110) surface discussed in Sec. IV in relation to the O_2^- spectrum include the atomic surface structure and electron energy-level scheme.

II. EXPERIMENTAL PROCEDURE

A Varian EPR spectrometer (V-4502) with 9-in. magnet was used with a cylindrical cavity operating in the TE 011 mode with a frequency of about 9.4 GHz. Signal-to-noise improvement was achieved by accumulating (continuously averaging) the spectrum using an NS-550 digital memory oscilloscope. Measurements were performed at -196 °C using a liquid-nitrogen-filled Dewar and between -150 °C and room temperature using a variable temperature apparatus (V-4557).

Accurate g values and widths were obtained by accumulating the spectrum with a marker of manganese (two peaks at $g = 1.9810$ and $g = 2.0328$ were used) or Li ($g = 2.0023$) and analyzing the spectra in digital form using an NS-400A data processor. Estimates of the number of spins were obtained by comparison with the Varian weak-pitch sample.

At room temperature, this could replace the specimen without moving the manganese marker (used as a sensitivity reference) which was fixed in the cavity. At low temperature, the Li dot attached to the outside of the Dewar or a small $CuSO_4$ crystal attached to the measuring tube served as an intensity reference.

The experimental procedure has been described previously.[11] The significant point is that the samples were prepared in uhv by crushing, and transferred to the measuring tube which was then lowered into the resonant cavity (and Dewar for low-temperature work) while continuously under uhv to reduce surface contamination. The residual pressure was less than 10^{-9} Torr, rising up to less than 10^{-8} Torr during crushing. Sorption and ion pumps were used to reduce carbon contamination during crushing.[12] Pure oxygen was admitted by heating an outgassed silver-diffusion leak in air. Residual gas analysis was performed with a quadrupole instrument (E. A. I. Quad 150 A).

Three types of GaAs have been used: (a) n-type oxygen and tellurium doped 300–1000 Ω cm; (b) n-type undoped $5\times10^{16}-5\times10^{17}$ carriers cm^{-3}; (c) p-type $1-5\times10^{19}$ carriers cm^{-3}. Also, low-resistivity p-type samples of GaSb, InAs, and GaP, and n-type AlSb and GaSb were measured. The samples were tested for resonances before crushing and none were found. (In some Te-O–doped GaAs samples, a broad background signal was present; these samples were not used.)

III. RESULTS

A. Clean-Surface Results

1. GaAs

All three types of GaAs showed a small approximately symmetric resonance at $g=2.0038\pm0.0003$ with a width of 9–10 G. Since the signal was only three to seven times the background signal due to the empty cavity and empty quartz tube, the shape of the line was not accurately determined. From a Brunauer-Emmett-Teller (B. E. T.) determination, the surface area of the powder was approximately 200 cm^2 and the number of spins from such a sample was 5×10^{13}. On cooling from 300 to 77 °K, the height of the signal was less than doubled and the width was unchanged.

Using accumulation, it was possible to measure a small change in this signal after adsorption of air, which suggests the signal is on or near the surface. In Fig. 1, the narrow signal marked Mn^{++} is the manganese marker signal used to monitor the over-all sensitivity of the cavity and the broad signal, S, is the surface signal from GaAs. In Fig. 1(a) the signals were recorded after 100 accumulations at 10^{-9} Torr. To test the reproducibility of such an accumulation two identical accumulations were stored and subtracted using the NS-400A data processor. Figure 1(b) shows that the result is close to zero, demonstrating that the result of an accumulation is reproducible. In Fig. 1(c) the result of 100 accumulations is shown after the vacuum system had been opened to the atmosphere without moving the sample or altering the cavity tuning. In Fig. 1(d) the spectra in parts (a) and (c) are subtracted using the NS-400A data processor. There is a small signal at the GaAs position after subtraction, indicating that the admission of air has reduced the GaAs signal. The over-all decrease in height is about 20%, with no change in width, and this has been found on four samples. The change was not reversed on pumping out the air and the total reduction in height becomes about 30% after exposure to air overnight. No change was observed after admission of pure oxygen to one sample at room temperature.

2. *Other Materials*

After crushing in vacuum, GaSb showed a signal with properties similar to GaAs: $g=2.0038\pm0.0004$, the width was approximately 9 G, and the number of spins was increased by less than a factor of 2 on cooling to 77 °K. This signal was reduced by about 20% on exposure to air.

No signal was found from InAs crystals crushed in vacuum. A small signal was found from AlSb powders but it has not been shown that this signal is sensitive to gases.

B. Oxygen Adsorption

1. GaAs

When the newly crushed powders of GaAs were cooled to 77 °K and exposed to oxygen a new signal (see Fig. 2) was obtained after an exposure of about 10^{-3} Torr min. The signal increased with exposure and reached a maximum before 1 Torr min. The line shape is that of a powder pattern of a species having an axially symmetric g tensor with $g_{\parallel}=2.036$ and $g_{\perp}=2.007$ (see Table I). As shown in Fig. 2, $g_{\parallel}$ was determined from the maximum of the absorptionlike peak and $g_{\perp}$ was calculated from the minimum (g_m) and the crossover (g_c) of the curve using the expression[14]

$$1/g_{\perp}=1/g_m-0.15\times2.28\,(1/g_m-1/g_c).$$

The low-field wing of the derivative curve can be fitted with a Lorentzian shape of width 40 G and the high-field wing with a width of 20 G. It is shown in Sec. IV that this signal is caused by the formation of negatively charged oxygen molecules, O_2^-, on the GaAs surface.

The maximum coverage (observed at 77 °K) corresponds to about 1×10^{16} spins or about 5% monolayer. The number of spins was determined by

numerically integrating the O_2^- signal and using the Li marker as a sensitivity reference.

After the maximum signal height had been achieved by exposures in excess of 1 Torr min, it was found that the height depended on the pressure. The maximum height occurs in a pressure of about 10^{-3} Torr oxygen. If the oxygen pressure is reduced the height is decreased by about 20%. If the pressure is increased above 5×10^{-3} Torr the signal height is decreased and the width is increased. The change in width can be monitored by fitting the wings of the line to a Lorentzian shape of appropriate width. This had increased from 20 to 30 G for the high-field wing when the signal height had reduced to one-quarter at a pressure of about 4×10^{-2} Torr. All these effects were reversible to changes in the oxygen pressure.

If a sample showing the O_2^- signal is warmed above $-100\,^\circ$C the signal disappears, and then reappears after recooling only if reexposed to oxygen. The signal width appeared to be independent of temperature.

The above results were obtained from both the high- and low-resistivity n-type GaAs, and the ratio of O_2^- signal to the clean surface signal was about the same in both cases. For experiments with p-type GaAs, the O_2^- signal was observed, with the same g values as for the n-type but the number of spins was reduced by an order of magnitude.

It was found that if the GaAs powders were first exposed to air, the O_2^- signal could not be observed even after outgassing at $200\,^\circ$C.

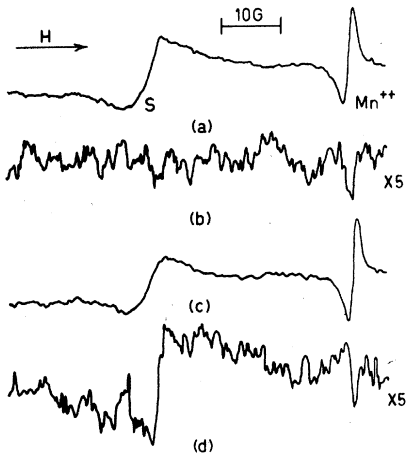

FIG. 1. Effect of exposure to air on the EPR, signal from the clean GaAs surface: (a) 100 accumulations of clean GaAs signal, S, and manganese marker signal Mn^{++}; (b) subtraction of two successive accumulations under vacuum (gain ×5); (c) 100 accumulations after admitting air to the system; (d) subtraction of spectrum (c) from (a) (gain ×5).

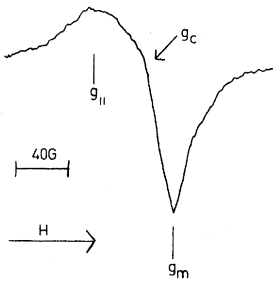

FIG. 2. EPR spectrum, at 77 °K and about 10^{-8} Torr oxygen, from uhv crushed GaAs after exposure to oxygen for 1 Torr min. The signal is attributed to O_2^- ions. Symbols defined in Table I.

2. AlSb *and Other Materials*

Powders of p-type GaP, GaSb, and InAs and n-type AlSb and GaSb were prepared in the same manner and exposed to oxygen at 77 °K. No signal was observed from the GaP, GaSb, or InAs surfaces under these conditions, even with a factor 10 increase in sensitivity after accumulation. A signal equal in height and width to the O_2^- signal on p-type GaAs would have been detected in these measurements, i.e., less than 0.5% monolayer. (The narrow lines around $g = 2.00$ and above due to gaseous oxygen in the measuring tube are clearly visible in these measurements and serve as a useful intensity reference which takes into account the sensitivity changes with different samples.) However, in the case of n-type AlSb, an O_2^- signal was observed after exposure to oxygen at 77 °K.

The asymmetric O_2^- line from AlSb is shown in Fig. 3. The g values were calculated as for GaAs and are shown in Table I. hfs is resolved in this line and tentatively identified with a nucleus of spin $\frac{5}{2}$. The lines near $g_{||}$ were all separated by 7 ± 1 G and near $g_\perp$ by 4.2 ± 0.3 G.

The O_2^- signal on AlSb first appears after about 5×10^{-5} Torr min. The signal depends on pressure and temperature in a manner similar to GaAs. The height is immediately reduced if exposed to oxygen above 5×10^{-3} Torr and is slowly decreased by about 20% when the oxygen is removed. The signal disappears on warming to room temperature but reappears after reexposure to oxygen at 77 °K. The signal height is found to be inversely proportional to the absolute temperature between $-150\,^\circ$C and about $-40\,^\circ$C after which the signal becomes smaller and is not visible at $0\,^\circ$C (cf. $-100\,^\circ$C for O_2^- on GaAs). This effect occurred whether oxygen was left in the sample tube, while changing the temperature, or was first pumped away.

IV. DISCUSSION

A. Clean-Surface Signal

A signal from the clean surface of GaAs has not been detected previously[9,10] and was only clearly visible in these experiments after accumulation.

Since the signals from GaAs and GaSb are affected by air, it is probable that the unpaired electrons are on or near the surface. The surface density of spins is very small for all the III-V materials studied, being greatest on GaAs for which it is 0.03% monolayer. Apparently the (110) and (111) surfaces of III-V materials (exposed by crushing) do not possess "dangling" bonds to the same degree as the (111) surfaces of Si.[1,2]

The low surface density makes it possible that the signal is not representative of the ideal surface but may be associated with surface defects such as steps, kink atoms, etc. Another possibility is that the signal is associated with surface states which would only need to have a low density to explain the limited band bending in GaAs.[15] The number of spins was found to be nearly independent of the absolute temperature, implying that the electrons interact strongly, and perhaps therefore, the second possibility may be more likely.

B. Adsorption of Oxygen at 77 °K

This section deals with the asymmetric line found on GaAs and AlSb after oxygen adsorption at 77 °K and is divided into five sections: (a) the EPR spectrum, identification of the species as O_2^- ions and the model of the adsorbed ion; (b) the hfs and surface wave function; (c) the g values; (d) computer simulation; and (e) the process of adsorption.

1. EPR *Spectrum*

The signals shown in Figs. 2 and 3 can be described by the following spin Hamiltonian:

$$\mathcal{H} = \mu_B \vec{S}\cdot\overleftrightarrow{g}\cdot\vec{H} + \vec{S}\cdot\overleftrightarrow{A}\cdot\vec{I} \,. \tag{1}$$

Here $\mu_B \overleftrightarrow{g}$ is a tensor which measures the interaction of the applied magnetic field $\vec{H}$ with an electron of effective spin $S = \frac{1}{2}$. $\overleftrightarrow{A}$ is a tensor which measures the interaction between the spin $\vec{S}$ and a nucleus with nuclear spin $\vec{I}$. Significant interaction

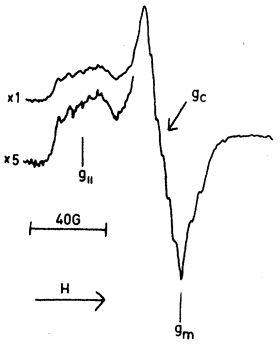

FIG. 3. The EPR spectrum at 77 °K and about 10^{-8} Torr oxygen of uhv crushed AlSb after exposure to oxygen for 1 Torr min. The signal is attributed to O_2^- ions. Symbols defined in Table I.

with a nucleus of spin $\vec{I}$ splits the electron energy level into $2I+1$ levels. In a powder this is reflected by the appearance of hfs near the principal g values although not all the $2I+1$ lines may be resolved at each point.

In the case of the GaAs powders no hfs is resolved, and only the components of the $\overleftrightarrow{g}$ tensor can be evaluated. However, the fact that $g_\parallel$ exceeds $g_\perp$ shows that the signal is caused by O_2^- ions on the surface, as seen below.

Since the signal is only present after oxygen adsorption, it must be due either to oxygen itself or a center on the surface made paramagnetic by the presence of oxygen. The fact that similar signals occur in the presence of oxygen on GaAs, AlSb, MgO,[4,6] ZnO,[4,5] SiO_2,[3] and zeolites,[7,8] makes the second hypothesis unlikely. Thus the signal must be due to one of the paramagnetic oxygen species with $S = \frac{1}{2}$ such as O^-, O_2^-, O_3^-, O^+, O_2^+. (In the anisotropic environment at the surface, O^0 and O_2 with $S = 1$ would not be paramagnetic.)

The fact that the radical forms most easily on n-type materials indicates that it must be one of the negatively charged species. Of these O^-,[16] and O_3^-,[17] have been observed with $g_\parallel < g_\perp$, which is to be expected on theoretical grounds. On the other

TABLE I. The g values and hyperfine splittings for O_2^- ions adsorbed on the (110) surface of GaAs and AlSb. The experimental g values were obtained from the powder pattern as indicated in Figs. 2 and 3 where g_c is g value at crossover and g_m the value at the sharp minimum. The hyperfine splitting K_1 is measured between the hyperfine lines at $g_\perp$, and K_3 is measured near $g_\parallel$. The parameters from the computer simulation are also provided.

	g values (±0.001)				Hyperfine constant (G)		
	g_m	g_c	$g_\perp$	$g_\parallel$	K_1		K_3
GaAs	2.002	2.017	2.007	2.036	• • •		• • •
AlSb	2.002	2.012	2.005	2.041	4.2±0.3		7±1
	g_{yy}	g_{xx}		g_{zz}	$A_{xx}/g\mu_\beta$	$A_{yy}/g\mu_\beta$	$A_{zz}/g\mu_\beta$
AlSb (from computer simulation)	2.002	2.005		2.041	4.4	4.4	6.4

hand O_2^- has been observed with $g_{\parallel} > g_{\perp}$ in the bulk of sodium and potassium superoxides[17] and lithium sulphate.[18] Since $g_{\parallel} > g_{\perp}$ for the present signal also, it is concluded that O_2^- is the radical observed. Experiments using oxygen enriched in O^{17} demonstrate that the species formed on the surface of MgO, also thought to be O_2^- ions, is indeed due to a diatomic ion.[6] Theoretically, the O_2^- spectrum is expected to possess three principal g values and this is usually the case, for example, in the bulk of alkali halides[19] and on the surface[4-8] of MgO, ZnO, and zeolites. The inability to resolve g_{xx} and g_{yy} at $g_{\perp}$ is explained by the large linewidth in the case of GaAs and AlSb. In the case of AlSb, it was necessary to assume two g values at $g_{\perp}$ to simulate the experimental spectrum (Sec. IV B 4).

Before discussing the g values and hfs in detail, some general features are considered. First, the hfs resolved in the case of AlSb must be due to interaction with a surface nucleus since oxygen does not have an abundant isotope with a nuclear spin. Both Al and Sb have a high nuclear spin and significant interaction with more than one nucleus would split the O_2^- signal into more than 20 lines near $g_{\parallel}$ and $g_{\perp}$. This however is not observed. Thus the O_2^- ion must lie close to a single surface atom.

Second, each O_2^- ion must occupy an identical, or nearly identical site. Otherwise, the different interactions experienced by the ions either differently oriented or on different sites would lead to a range of g values and hyperfine splittings. In the case of O_2^- on GaAs where no hfs was resolved, the large linewidth could perhaps be caused by the occupation of slightly different sites. Molecular rotation about the symmetry axis is discounted because distinct x and y components of the g tensor are required to fit the computed spectrum.

2. *Hyperfine Structure*

Analysis of the hfs provides information about the wave function of the unpaired electron. The following discussion is carried through for O_2^- ions adsorbed on AlSb near a single surface atom, following the model in Sec. IV B 1. From the results of the computer simulation in Sec. IV B, this surface atom must be Al and not Sb.

The interaction of the surface Al nucleus with the unpaired electron entirely localized on the O_2^- ion is too small to explain the observed splittings. Assuming that the separation of the Al nucleus and the O_2^- ion is about 2 Å, the splitting would be only about 0.2 G compared with the experimental values of 4.2 and 7 G. Thus the unpaired electron must be partially localized in a surface orbital which we assume is a hybrid orbital composed of s and p wave functions. As a first approximation we assume the wave function $\psi(r)$ of the unpaired electron is

$$\psi(r) = c_1\ \phi_0(r) + c_2\,[\alpha\ \phi_s\ (r) + \beta\ \phi_p(r)], \tag{2}$$

where $\phi_0(r)$ is the wave function of the extra electron on O_2^- in the absence of neighboring atoms, $\phi_s(r)$ and $\phi_p(r)$ refer to the s and p components of the Al surface-atom wave functions, which are assumed to contribute a fraction $(c_2)^2$ to the wave function of the unpaired electron, α^2 and β^2 are the fractions of s and p contributions, respectively, and

$$\alpha^2 + \beta^2 = 1\ . \tag{3a}$$

Neglecting overlap among ϕ_0, ϕ_s, and ϕ_p,

$$(c_1)^2 + (c_2)^2 = 1\ . \tag{3b}$$

Assuming the electron occupies the wave function in Eq. (2), the components of the hyperfine tensor $\vec{A}$ [see Eq. (1)] are made up of two parts. The isotropic s-orbital contribution a and the anisotropic p-orbital part b are given by

$$a = \tfrac{8}{3}\pi\ g g_N \mu_\beta\ \mu_N (c_2)^2\ \alpha^2 \left|\ \phi_s(0)\ \right|^2, \tag{4a}$$

$$b = \tfrac{2}{5} g g_N \mu_\beta \mu_N (c_2)^2 \beta^2 \langle r^{-3} \rangle, \tag{4b}$$

where μ_β and μ_N are the Bohr and nuclear magnetons and g and g_N are the electron and nuclear g values. The quantity a depends on the wave function of the electron evaluated at the nucleus causing the hfs. The contribution to this from the oxygen wave function is negligible. Similarly, $\langle r^{-3} \rangle$, the expectation value of r^{-3} about the above-mentioned nucleus, is taken as $\langle \phi_p(r) | r^{-3} | \phi_p(r) \rangle$ for the same reason.

It is shown in Appendix A that the measured hyperfine splittings place restrictions on the possible values of a and b and therefore on α^2, β^2, and $(c_2)^2$. Making no assumptions about the orientation of the molecule near the surface atom, the maximum and minimum values of α^2 and the corresponding values of β^2 and $(c_2)^2$ can be calculated. The results from Appendix A are shown in Table II. The "probable minimum" in Table II is a result of further restrictions placed on a and b by the computer simulation results. The values of α^2 calculated for the possible minimum require values of a and b for which a computer fit was not obtained.

From these results it is concluded that the surface wave function of the Al atom adjacent to the molecule ion on the (110) surface of AlSb is largely p-like. The following assumptions are involved in this conclusion. (i) The unpaired electron from the O_2^- spends part of its time in an s-p hybrid surface wave function. (ii) The hybridization of this wave function is not much changed by the presence of the O_2^- ion.

3. *g Values*

The unpaired electron in the O_2^- ion occupies one of the antibonding π_g orbitals which are degenerate

in the free state. ($\pi_g = p^1 - p^2$, where p^1 refers to a p orbital orthogonal to the molecular axis, centered on atom 1 of the molecule.) After adsorption the symmetry about the molecular axis (taken as the z axis) is removed by the electric field gradient due to the crystal and/or covalent bonding with surface atoms.[20] In this case the orbital levels are split and the acquired unpaired electron occupies the orbital with higher energy (the y direction is taken parallel to the direction of this orbital).

The g-value expressions for the O_2^- ion in a field of orthorhombic symmetry have been derived by Känzig and Cohen.[21,19] The symmetry of an adsorption site on an undistorted (110) surface of a III-V compound is not orthorhombic, but could be monoclinic or triclinic. In a field of triclinic symmetry the g-value expressions could differ from those for orthorhombic symmetry and calculations show that both g_{xx} and g_{yy} can exceed the free-electron value g_e. In the case of oxygen interaction with zeolites,[7,8] interpreted as O_2^- adsorption, both g_{xx} and g_{yy} do exceed g_e. In the expression of Känzig and Cohen however, g_{yy} is essentially equal to g_e. In the present case of O_2^- on AlSb and GaAs, $g_{yy} = g_e$ and the g-value expressions[21] of Känzig and Cohen may be applicable. Ignoring higher-order terms, these are

$$g_{xx} = g_e + 2\lambda/E, \quad g_{yy} = g_e, \quad g_{zz} = g_e + 2\lambda/\Delta,$$

where Δ is the separation of the π_g levels, and E is the separation between the σ_g level ($\sigma_g = p_x^1 - p_x^2$) and the π_g level occupied by the unpaired electron. The spin-orbit coupling constant λ is taken as 0.014 eV[7] for O_2^-. From the measured g values (see Table I) and the above expressions, it is found that $\Delta = 0.7$ eV and $E = 3.2$ eV for O_2^- on AlSb and $\Delta = 0.8$ eV and $E = 3.6$ eV (assuming $g_{xx} = g_c$) for O_2^- on GaAs.

The term in the crystal field expansion, which splits the π_g levels, is proportional to $(\partial^2 V/\partial x^2 - \partial^2 V/\partial y^2)$. If the splitting is entirely due to the field from the crystal, the value of $(\partial^2 V/\partial x^2 - \partial^2 V/\partial y^2)$ is about 5×10^{19} V m^{-2} for O_2^- on AlSb and 6×10^{19} V m^{-2} for O_2^- on GaAs. These gradients are averages of the values through each of the oxygen atoms in the molecule.

The electric field gradient at the surface is expected to affect the energy-level separations in all adsorbed atoms and molecules whether or not they are paramagnetic. These energy shifts may have an effect on the positions of surface Auger electron transitions in which there is a great deal of interest at present.[22] The above values of the field gradient could be used to estimate the size of this effect.

TABLE II. Extrema values of the s-p hydridization of the Al surface orbital, occupied by the unpaired electron from O_2^-, which are compatible with the observed hyperfine splittings. α^2 is the fraction of s wave function, β^2 is the fraction of p wave function and $(c_2)^2$ is the total contribution of the surface orbital to the unpaired electron wave function.

Extremum of α^2 for Al	α^2	β^2	$(c_2)^2$
Unqualified maximum	0.10	0.90	0.04
Probable minimum	0.06	0.94	0.06
Possible minimum	0.02	0.98	0.12

4. *Computer Simulation*

To test whether the model proposed in Sec. IV B 1 was compatible with the experimental results, the powder spectra of O_2^- on AlSb and GaAs were simulated on a computer within the framework of the model. The spin Hamiltonian used to describe the spectrum is given in Eq. (1). We can refer the vectors and tensors in this equation to a system of coordinates x, y, z in which the $\overleftrightarrow{g}$ tensor is diagonal with principal components g_{xx}, g_{yy}, and g_{zz}. The z axis is taken parallel to the internuclear axis and x and y are taken along the π orbitals of the O_2^- ion. The hyperfine interaction tensor $\overleftrightarrow{A}$ is not necessarily also diagonal in this coordinate system, i.e., its principal axes need not be parallel to x, y, z. As described in Sec. IV B 2, we assume the hyperfine structure occurs when the electron occupies the s-p hybrid wave function on the surface atom. Then $\overleftrightarrow{A}$ has axial symmetry about the s-p hybrid orbital with principal components $A_{XX} = A_{YY} = a - b$ and $A_{ZZ} = a + 2b$, where a and b are defined in Eq. (4). The X, Y, Z system of coordinates is chosen so that the Z axis is parallel to the s-p orbital axis. The principal axes of the $\overleftrightarrow{A}$ tensor (X, Y, Z) and the $\overleftrightarrow{g}$ tensor (x, y, z) will not be parallel unless the s-p surface orbital is parallel to the π or σ bonds of the O_2^- ion and this has not been assumed in what follows. The case of nonparallel $\overleftrightarrow{A}$ and $\overleftrightarrow{g}$ tensors has rarely been considered.[23,24]

Since the $\overleftrightarrow{A}$ tensor is axially symmetric, the orientation of the two principal axis systems can be specified by two angles ϕ and θ. As shown in Fig. 4, θ is the angle between the z and Z axes which are chosen so that $\theta < \pi/2$, and ϕ is the angle between the y and Y axes. The components of the $\overleftrightarrow{A}$ tensor in the x, y, z system of coordinates are

$$A_{xx} = (a - b) + 3b \sin^2\theta \cos^2\phi ,$$

$$A_{xy} = A_{yx} = 3b \sin^2\theta \cos\phi \sin\phi ,$$

$$A_{xz} = A_{zx} = 3b \sin\theta \cos\theta \cos\phi ,$$

$$A_{yy} = (a - b) + 3b \sin^2\theta \sin^2\phi ,$$

$$A_{yz} = A_{zy} = 3b \sin\theta \cos\theta \sin\phi ,$$

$$A_{zz} = (a - b) + 3b \cos^2\theta \ .$$

The energy E_0 absorbed in an ERP transition

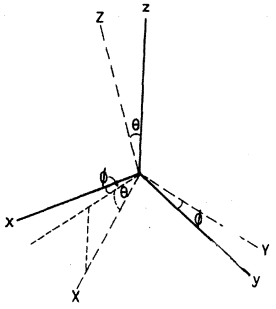

FIG. 4. Reference system of axes: x, y, z is the principal system of axes for the g tensor and X, Y, Z is the principal system of axes for the A tensor. Since A is axially symmetric about Z, Y can be chosen in the xy plane. The Euler angles θ and ϕ are shown.

($\Delta m_s = \pm 1$, $\Delta m_I = 0$) can be obtained from Eq. (1) using first-order perturbation theory

$$E_0 = g\mu_\beta H + Km_I \,, \tag{5}$$

where

$$g^2 = g_{xx}^2 l^2 + g_{yy}^2 m^2 + g_{zz}^2 n^2$$

and[24]

$$K^2 g^2 = (A_{xx} l g_{xx} + A_{xy} m g_{yy} + A_{xz} n g_{zz})^2 + (A_{yx} l g_{xx} + A_{yy} m g_{yy} + A_{yz} n g_{zz})^2 + (A_{zx} l g_{xx} + A_{zy} m g_{yy} + A_{zz} n g_{zz})^2 .$$

If α and β are the spherical polar angles made by the applied magnetic field H with respect to the z and x axes, $l = \cos\beta \sin\alpha$, $m = \sin\beta \sin\alpha$, and $n = \cos\alpha$.

The powder spectrum was determined using an algorithm given by Griscom *et al.*[25] First, the resonant field was calculated from Eq. (5) for a range of α and β and histogrammed using a PDP-8/L computer. Since all solid angles are equally likely in a powder, equal increments in $\cos\alpha$ and in β were used. From Eq. (5) all values of the resonant field are included if $0 \le \alpha \le \pi/2$ and $0 \le \beta \le 2\pi$ and 90 values of $\cos\alpha$ and of β were used in each of the four quadrants of this half-sphere.

The histogram gives the relative number $N(H_i)$ of species resonant at field H_i in the histogram interval ΔH. The derivative of the total adsorption at H_j, $D(H_j)$, was found by convoluting the histogram with the derivative $L(H)$ of a line shape of appropriate width W. Thus

$$D(H_j) = \sum_i N(H_i)\, L(H_j - H_i)\, \Delta H.$$

Both Lorentzian and Gaussian line shapes were used. Generally, 80 values of $D(H_j)$ were evaluated over the range of the experimental spectrum and ΔH was chosen so that $4\,\Delta H < W$.

In simulating the O_2^- spectrum from AlSb, it was first assumed the electron interacted with an Al nucleus which has $I = \frac{5}{2}$. Good agreement was obtained between the experimental and calculated curves assuming the $\overleftrightarrow{A}$ and $\overleftrightarrow{g}$ tensors are parallel (see Fig. 5). In this simulation the linewidth was taken as 2.3 G and a Lorentzian shape was used. The heights of the peaks at g_{zz} on the simulated curve are too large, indicating a larger linewidth is required there. The increased linewidth at g_{zz} is thought to be caused by a distribution of values of g_{zz} from O_2^- ions adsorbed at slightly different sites. The value of g_{zz} is expected to be much more sensitive to slight changes in environment than g_{xx} and g_{yy}.

It was found from the simulations that different values of g_{xx} and g_{yy} were needed to fit the experimental results. A single $g_\perp$ value might be expected from a cursory inspection of Fig. 3, but was inadequate. The experimental spectrum could also be fitted when the angle θ between the Z axis of the $\overleftrightarrow{A}$ tensor and the z axis of the $\overleftrightarrow{g}$ tensor was increased up to 30°. It is shown in Appendix A that, within the framework of the model, $0 \le \theta \le 40°$ and $\phi = 45°$ if $\theta \neq 0$ and only this range of angles was used in the simulations (see Fig. 6).

Attempts to fit the experimental curve assuming that the unpaired electron interacted with an Sb nucleus, rather than an Al nucleus, were unsuccessful. Too many lines resulted from interaction with the two different Sb isotopes ($I = \frac{5}{2}$, 57% abundant and $I = \frac{7}{2}$, 43% abundant) which have nuclear g values in the ratio 1.85 : 1. This means the hyperfine lines due to each isotope cannot overlap to produce the five- or six-line spectrum observed experimentally. This was also found when the $\overleftrightarrow{A}$ and $\overleftrightarrow{g}$ tensors were taken as nonparallel.

In the case of O_2^- adsorbed on GaAs, the spectrum is so featureless that it could be fitted satisfactorily in a variety of ways. In particular, it could not be determined whether unresolved hyperfine splitting was present or not.

From the simulation, we conclude that the model proposed in Sec. IV B 1 is indeed compatible with the experimental spectrum. For O_2^- on AlSb,

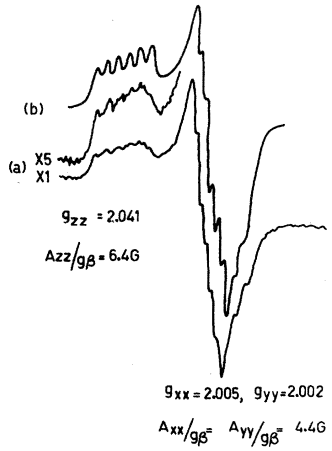

FIG. 5. EPR signal for O_2^- ions on AlSb: (a) experimental spectrum; (b) computed spectrum using the g values and hyperfine constants shown and a Lorentzian "single-crystal" linewidth of 2.3 G.

the hfs is not sufficiently well resolved to distinguish between different orientations of the principal axes of the $\vec{A}$ and $\vec{g}$ tensors but the angle between the molecular axis (z axis) and the s-p hybrid orbital (Z axis) is probably less than 30°.

5. *Adsorption Process*

The adsorption process must involve at least two steps,

$$O_2(\text{gas}) \rightleftharpoons O_2(\text{ads}), \tag{6a}$$

$$O_2(\text{ads}) + Y \rightleftharpoons O_2^- + Y^+ + \text{energy}. \tag{6b}$$

In Sec. IV B 1 it has been assumed that Y is more likely the group-III atom or possibly a small group of nearby atoms. This is inferred from the hfs and the fact that the O_2^- must be closely associated with a surface positive charge, forming a surface dipole layer. If the O_2^- constituted a net negative charge on the surface, the electrostatic energy needed to transfer an electron through the resulting space-charge region would prohibit coverages as great as observed[26] (about 5% monolayer). This view is supported by the $g_{\parallel}$ values of the O_2^- on GaAs and AlSb, which are about the values expected for O_2^- near a single positive charge.[7,8]

Since electron transfer takes place from the surface to the adsorbed molecule, the highest occupied electron energy levels of the O_2^- ion must lie below or close to the Fermi level after adsorption. However, the Fermi level of n-type GaAs lies more than 4 eV below the vacuum level, while the electron affinity of O_2^- is only about 0.5 eV.[6] Thus the upper energy levels of the O_2^- molecule must be lowered by about 4 eV by interaction with the crystal (as shown in Fig. 7).

Adsorption will proceed until electrostatic repulsion between the surface dipoles raises the O_2^- level above the Fermi level. Thus the coverage is expected to be greater on n-type than on p-type materials. In fact, the coverage on p-type GaAs was found to be an order of magnitude less than on n type. These considerations may explain why no O_2^- formation was observed on p-type GaP, GaSb, and InAs. However, O_2^- may not form even on n-type GaSb and InAs because unlike GaAs and AlSb the Fermi level is believed to be pinned close to the valence band.[27] In agreement with this, experiments on n-type GaSb indicate no O_2^- formation.

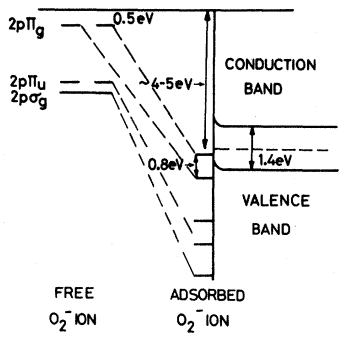

FIG. 7. Schematic diagram of the uppermost electron energy levels of GaAs and of O_2^- before and after adsorption. The labeling of the energy levels and the changes in energy-level separations in the O_2^- after adsorption are explained in Sec. IV B 3.

The disappearance of the O_2^- signal on warming to − 100 °C for GaAs (0 °C for AlSb) means that the molecule is only weakly held. Because the signal does not reappear on recooling, the oxygen must desorb at these temperatures or perhaps dissociate or diffuse into the bulk. Since the O_2^- signal can be obtained repeatedly by reexposure to oxygen at low temperatures the adsorption sites are not destroyed by the change at − 100 °C (0 °C for AlSb). Thus the simplest hypothesis is that the oxygen molecule desorbs at the temperature at which the signal disappears. A possible mechanism is that the "physisorbed" O_2 molecule is desorbed at these temperatures. The number of O_2^- ions will then be depleted as the equilibrium in Eq. (6b) is maintained.

After the formation of O_2^- is stopped by electrostatic repulsion between the dipoles, further oxygen adsorption must be nonparamagnetic since no further EPR signal is observed. Rosenberg *et al.*[28] have found that on vacuum-crushed GaAs at 77 °K, oxygen forms half a monolayer coverage after exposures of about 500 Torr min. This is "irreversible" to pumping, but not to warming. In addition, there is a further reversible adsorption which could be pumped off at 77 °K. The reversibly adsorbed oxygen could be the explanation of the decrease in the signal height and increase in width at high pressures (about 10^{-2} Torr of oxygen) observed for the O_2^- EPR signal, due to strong dipole interactions, competition for surface sites, or shortening of spin-lattice relaxation times.

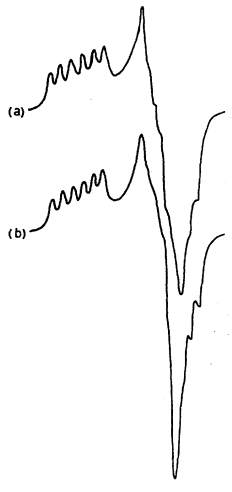

FIG. 6. Computed spectra of O_2^- ions on AlSb assuming nonparallel principal axes of A and g tensors: (a) angle between molecular axis and undistorted sp hybrid axis, $\theta = 30°$; (b) $\theta = 40°$. The angle φ (see Fig. 4) is 45°. In both cases Lorentzian line shapes were used. Compare these curves with Fig. 5(b), corresponding to $\theta = 0$. This illustrates the effects of assuming various angles between the principal axes.

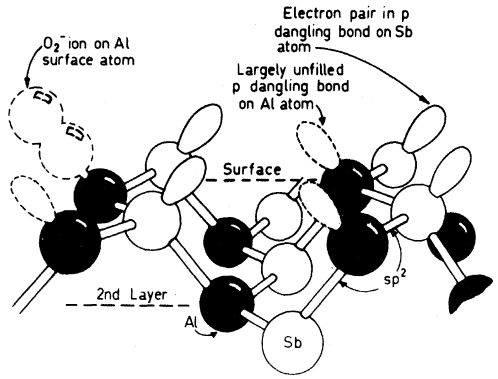

FIG. 8. Diagram of the proposed model of the (110) surface of the III-V compounds. The nearest-neighbor bonds of the surface atoms are sp^2-like. The dangling orbital of the group-III atom is p-like and empty while that of the group-V atom is p-like and occupied by a pair of electrons. The group-III atom is expected to be displaced towards the bulk along the dangling bond axis (movement not shown). An adsorbed O_2^- ion is shown schematically on an Al surface atom.

C. Structure of (110) Surface of III-V Compounds

Some proposals have been made concerning the structure of (110) III-V compound surfaces. On the basis of LEED (low-energy electron diffraction) spot intensity asymmetries, MacRae and Gobeli[29] suggested that the surface atoms were shifted from their ideal positions, while preserving the ideal two-dimensional unit cell size. It was suggested that the group-III atoms (metal atoms) were shifted vertically out of the surface plane, while the group-V atoms (nonmetal atoms) were shifted inward. An opposite conclusion was reached by Levine and Freeman[30] on the basis of surface-state band calculations, adjusted to fit measured surface electrical properties. They used a largely ionic model of the structure and assigned s orbitals to the M (metal) ion sites, and p_x, p_y, p_z orbitals to the X (nonmetal) ion sites. The appearance of M-like surface states in their model was facilitated by a rotation of the surface structure and an expansion, the net effect of which was to move the M ions up from the surface plane and the X ions down from it.

The present EPR results show that indeed there are strongly p-like orbitals on the surface. However the evidence points to their being associated with the M atoms (Al), whereas Levine and Freeman associate s orbitals with the M atoms. The latter treatment however was worked out in detail for zinc blende, for which II-VI compound a simple ionic M^{++} X^{--} model is more applicable. Furthermore, a number of assumptions were necessary to carry through the calculation. Therefore, it may not have close application to the present III-V compounds.

Two major features stand out from the EPR results. First, the presence of p-like orbitals on M atoms, referred to above. Second, the failure to detect a strong unpaired electron signal from the clean surfaces. The latter suggests that the simple picture of an ideal (110) surface with one unpaired bond per surface atom needs modification, otherwise a strong EPR signal would be expected, cf. silicon.[1,2] Line broadening effects in such an arrangement would normally be counteracted by exchange narrowing, but, in principle, one could not rule out the possibility of sufficiently strong broadening being present to make the resonance undetectable. However the simplest solution is that the $\frac{3}{4}$ electron ideally associated with the dangling bond on the M atom[31,32] is transferred to the $\frac{5}{4}$ electron ideally associated with the dangling bond on the X atom. This gives a dangling electron pair on the X atom and no dangling electron on the M atom, and hence no EPR signal is expected. This type of suggestion was advanced earlier by Gatos and Lavine[33] principally for (111) surfaces of III-V compounds. In the case of a (111) surface, the surface atoms are all of one chemical species, and the applicability of the proposal of electron transfer can be questioned.[31,32] However, in the present case of (110) surfaces, adjacent atoms are of alternate M and X type, and the process of electron transfer could take place more readily.

Taking this suggestion into account, together with the evidence of a mostly unfilled dangling p-like orbital on the M atom, it is possible to make a specific proposal for a (110) surface. This is presented merely as one simple model that is consistent with the data. The true structure may be much more complicated.

Referring to Fig. 8, which shows a view of a (110) surface, the bonds in the surface plane are of mainly sp^2 hybrid type, as are the bonds to the second layer. The dangling largely empty bond on the M atom is of type p. The two-electron filled dangling bond on the X atom is also of type p. These assignations were made to be consistent with the original normalization, as well as keep the bond angles reasonable. Thus the free M atom content of s^2p^1 filled, is preserved as s^1p^2. In the case of the X atom the normalization is equivalent to three bonds composed of (s, p_i, p_j), where i, j, k are the three orthogonal p directions, together with an electron pair in a p_k orbital.

Although pure sp^2 bonds are coplanar, a distortion from the plane containing the two in-surface neighbors, and the second-layer neighbor, is required in order for the surface to be not too different from the ideal structure, i.e., the surface atom is not pulled completely into the plane composed of the three neighbors [this plane is at an angle to the (110) surface]. In the case of the X

atom, its three nearest-neighbor bonds and dangling bond, each contain two electrons. Therefore, by the principle of pair repulsion, some equivalence of the four bond angles could be expected, and hence the angles may not differ greatly from tetrahedral. This would keep the X atom near its "ideal" position. The M atom has no dangling electron pair and hence would be pulled down more than the X atom, to an extent depending on the degree of purity of sp^2 character of the three nearest neighbor bonds. Note that the direction of pull is normal to, and towards, the base composed of these neighbors, which is at an angle to the surface. [This is best envisaged by looking at a three dimensional model of a (110) surface.]

It is noted that the lowering of the M atom relative to the X atom would agree with MacRae and Gobeli's[29] conclusion from a kinematical analysis of the LEED data. However, pending a more accurate LEED analysis, we do not attach very much significance to this agreement at this stage. It is also noted that a rehybridization of surface wave functions is suggested by the ion neutralization studies of Pretzer and Hagstrum.[34] The above model is speculative, but is presented to illustrate one way of tying up the data with a specific possibility.

D. Adsorption Site

It was shown in Sec. IV B 2 that the O_2^- ion adsorption site on AlSb is adjacent to an Al surface atom. In this case the hyperfine spectrum is explained by partial participation of the unpaired electron π_g orbital from the O_2^- ion in the s-p hybrid orbital on the Al atom. If the molecular axis were parallel to the s-p orbital axis, the Al-O_2^- complex would possess $C_{\infty v}$ symmetry and the Al s-p orbital would not contribute the to π orbitals of the O_2^- ion. The electric field due to the crystal would decrease this symmetry and mix the s-p orbital and π orbital to some extent. However a calculation shows that this is not sufficient to explain the size of the hyperfine splitting with the Al nucleus. Thus the molecule axis must be oriented in some other direction than parallel to the s-p band orbital axis.

A further restriction can be found. Since the hyperfine splittings at g_{xx} and g_{yy} are about equal, analysis in Appendix A shows that the molecular axis must make an angle of less that 40° with the Al s-p orbital axis. Since this orbital ideally makes an angle of 55° with the surface, the molecule would not be oriented parallel to the surface.

V. SUMMARY

The main conclusions which can be drawn from this investigation are summarized.

(a) A number of paramagnetic centers have been detected for the first time on the clean surfaces of GaAs and GaSb. The small signal found (about 3×10^{11} spins cm^{-2}) must come from the surface region since it is affected by air. Because it is so small, less than 1 spin/1000 surface atoms, it might be associated with certain surface irregularities or with surface states. Certainly no EPR signal corresponding to the broken bond associated with each surface atom was detected. To explain this fact a model has been proposed in which the electrons are paired in the broken orbital associated with the group-V element, leaving the orbital on the group-III element empty.

(b) After adsorption of oxygen on the surfaces of GaAs and AlSb at low temperatures, a new signal was obtained. The nature of the EPR signal allowed the species producing the spectrum to be positively identified as O_2^- ions.

(c) From the hyperfine structure, observed from O_2^- on AlSb, it is found that the unpaired electron is about 5% localized in an Al orbital. This orbital is at least 90% p-like. It is considered as being the empty broken orbital on the Al surface atom. In this case, the nearest-neighbor bonds of the Al-surface atoms would be sp^2-like. From a model it is deduced that the Al atom would be lowered with respect to the Sb atom.

ACKNOWLEDGMENTS

The authors thank Professor R. M. Golding for deriving Eq. (5) in the text, and D. Heron for writing the computer program used in the simulation. Support from the Australian Research Grants Committee and the U. S. Army Research and Development Group (Far East) is gratefully acknowledged.

APPENDIX: HYPERFINE INTERACTION WITH A SURFACE NUCLEUS

In Sec. IV B 2 it was assumed that the unpaired electron occupied the wave function

$$\psi(r) = c_1\,\phi_0(r) + c_2[\alpha\phi_s(r) + \beta\phi_p(r)],$$

where $(c_2)^2$ is the fraction of surface wave function made up from an Al orbital of fraction α^2, s type and β^2, p type. It is possible to estimate α^2 and β^2 from the values of the hyperfine splittings which depend on a and b. From Eq. (4), $a \propto (c_2)^2\alpha^2$ and $b \propto (c_2)^2\beta^2$. As noted, a and b cannot be uniquely deduced because it is not permissible to make the usual assumption that the principal axes of the $\overleftrightarrow{A}$ and $\overleftrightarrow{g}$ tensors are parallel. Therefore the extreme values of a and b are found from the experimental splittings. The results of the computer simulation are then used to further reduce the likely range of α and β.

The peaks in the powder spectrum occur when the field lies along the principal axes of the $\overleftrightarrow{g}$ tensor. If the hyperfine splitting near $g_{zz}(g_{\parallel})$ is K_3 then using the expressions in Sec. IV B 2,

$$K_3^2 = A_{xx}^2 + A_{yx}^2 + A_{zx}^2 = (a-b)^2 + 3\cos^2\theta\,(b^2+2ab)\ . \tag{A1a}$$

Similarly, the hyperfine splittings at g_{xx} (K_1) and at $g_{yy}(K_2)$ are found to be

$$K_1^2 = (a-b)^2 + 3\,\sin^2\theta\cos^2\phi\,(b^2+2ab), \tag{A1b}$$

$$K_2^2 = (a-b)^2 + 3\sin^2\theta\,\sin^2\phi\,(b^2+2ab)\ , \tag{A1c}$$

where θ and ϕ are the interaxis angles (Fig. 4).

The experimental values of K_1, K_2, and K_3 are given in Table I ($K_1 = K_2 = 4.2$ G and $K_3 = 7$ G). These values restrict the range of possible values of θ and ϕ. Since $K_1 = K_2$, inspection of Eqs. (A1) shows that either $\theta = 0$, π or $\phi = \frac{1}{4}\pi$, etc. (since $b \neq -2a$ as a and b have the same sign, and $b \neq 0$ as $K_3 \neq K_1$). Also from Eqs. (A1) it can be shown that

$$(a-b)^2 = \frac{K_3^2 - (K_1^2 + K_2^2 + K_3^2)\cos^2\theta}{1 - 3\cos^2\theta} \tag{A2a}$$

and

$$b^2 + 2ab = \frac{2K_3^2 - K_1^2 - K_2^2}{9\cos^2\theta - 3}\ . \tag{A2b}$$

Since the left-hand side of the above equations must be positive (a and b have the same sign), $\cos^2\theta > \frac{1}{3}$ and also $\cos^2\theta > K_3^2(K_1^2 + K_2^2 + K_3^2)^{-1}$.

We can now determine the extremum values of α^2, the degree of s hybridization of the surface orbital. From Eqs. (3) and (4), $(a-b)$ is proportional to α^2 for a given contribution $(c_2)^2$, of the surface orbital to the unpaired electron wave function. From Eq. (A2a), $(a-b)$ has a maximum when $\theta = 0°$ and a minimum when $\theta = 40°$ (which is the maximum allowed value of θ). Substituting these values in Eqs. (A1), the maximum value of α occurs when $a \approx 5.1$ G and $b \approx 0.9$ G and the "minimum possible" value of α^2 occurs when $a = b \approx 3.1$ G. However the greatest value of θ, which gave a reasonable fit to the experimental data using computer simulation, was 30° which leads to $a \approx 4.8$ G and $b \approx 1.6$ G for the condition of minimum probable value of α^2.

Using values[35] of $|\phi_s(0)|^2 = 20.4 \times 10^{24}$ cm^{-3} and of $\langle r^{-3}\rangle = 8.95 \times 10^{24}$ cm^{-3} for Al in Eqs. (4) the values of α^2, β^2, and $(c_2)^2$ given in Table II are found from the above values of a and b.

---

*Research supported by the U. S. Army Research and Development Group (Far East) Dept. of the Army under Grant No. DA-CRD-AFE-592-544-69-G154 and by the Australian Research Grants Committee.

[1]M. F. Chung and D. Haneman, J. Appl. Phys. 37, 1879 (1966).

[2]D. Haneman, Phys. Rev. 170, 705 (1968).

[3]G. Hochstrasser, J. F. Antonini, and I. Peychès, in *The Structure and Chemistry of Solid Surfaces*, edited by G. A. Somorjai (Wiley, New York, 1969), p. 36-1.

[4]J. H. Lunsford and J. P. Jayne, J. Chem. Phys. 44, 1487 (1966).

[5]R. D. Iyengar, V. V. Subba Rao, and A. C. Zettlemoyer, Surface Sci. 13, 251 (1969).

[6]A. J. Tench and P. Holroyd, Chem. Commun. 471 (1968).

[7]P. H. Kasai, J. Chem. Phys. 43, 3322 (1965).

[8]K. M. Wang and J. H. Lunsford, J. Phys. Chem. 73, 2069 (1969).

[9]G. K. Walters and T. L. Estle, J. Appl. Phys. 32, 1854 (1961).

[10]P. Chan and A. Steinemann, Surface Sci. 5, 267 (1966).

[11]D. J. Miller and D. Haneman, Surface Sci. 19, 45 (1970).

[12]D. J. Miller and D. Haneman, Surface Sci. 24, 639 (1971).

[13]G. A. Wolf, in *Compound Semiconductors, Vol. I. Preparation of III-V Compounds*, edited by R. K. Willardson and H. L. Goering (Reinhold, New York, 1962), Chap. 3.

[14]J. W. Searl, R. C. Smith, and S. J. Wyard, Proc. Phys. Soc. (London) A78, 1174 (1961).

[15]J. Van Laar and J. J. Scheer, Surface Sci. 8, 342 (1967).

[16]B. Segall, G. W. Ludwig, H. H. Woodbury, and P. D. Johnson, Phys. Rev. 128, 76 (1962).

[17]J. E. Bennett, D. J. E. Ingram, and D. Schonland, Proc. Phys. Soc. (London) A69, 556 (1956).

[18]C. L. Aseltine and Y. W. Kim, J. Phys. Chem. Solids 29, 531 (1968).

[19]H. R. Zeller and W. Känzig, Helv. Phys. Acta 40, 845 (1967).

[20]C. L. Gardner, J. Chem. Phys. 46, 2991 (1967).

[21]W. Känzig and M. H. Cohen, Phys. Rev. Letters 3, 509 (1959).

[22]J. J. Uebbing and N. J. Taylor, J. Appl. Phys. 41, 804 (1970).

[23]R. Lefebvre and J. Maruani, J. Chem. Phys. 42, 1480 (1965).

[24]R. M. Golding (unpublished).

[25]D. L. Griscom, P. C. Taylor, D. A. Ware, and P. J. Bray, J. Chem. Phys. 48, 5158 (1968).

[26]D. O. Hayward and B. M. W. Trapnell, *Chemisorption* (Butterworths, London, 1964), p. 263.

[27]J. D. Levine, J. Vac. Sci. Technol. 6, 549 (1969).

[28]A. J. Rosenberg, J. N. Butler, and A. A. Menna, Surface Sci. 5, 1 (1966).

[29]A. U. MacRae and G. W. Gobeli, J. Appl. Phys. 35, 1629 (1964).

[30]J. D. Levine and S. Freeman, Phys. Rev. B 2, 3255 (1971).

[31]D. Haneman, in *Proceedings of the International Conference on the Semiconductors, Exeter*, 1962 (The Institute of Physics and the Physical Society, London, 1962), p. 842.

[32]D. B. Holt, J. Appl. Phys. 31, 2231 (1960).

[33]H. C. Gatos and M. C. Lavine, J. Electrochem. Soc. 107, 427 (1960).

[34]D. D. Pretzer and H. D. Hagstrum, Surface Sci. 4, 265 (1966).

[35]G. D. Watkins and J. W. Corbett, Phys. Rev. 134, A1359 (1964).